Nanoparticles

DOI: 10.1002/ange.201103002

Palladium Concave Nanocubes with High-Index Facets and Their Enhanced Catalytic Properties**

*Mingshang Jin, Hui Zhang, Zhaoxiong Xie, and Younan Xia**

Palladium nanocrystals have been actively explored in recent years due to their unique properties and applications related to catalysis.[1] Like other systems, the catalytic activity of Pd nanocrystals is strongly dependent on both size and shape, with the shape playing a more important role in determining the selectivity. Over the past decade, Pd nanocrystals have been prepared in a variety of different shapes, with notable examples including cube, octahedron, decahedron, icosahedron, plate, rod, and bar that are typically enclosed by low-index facets such as {111}, {100}, and {110}.[2] In comparison, synthesis of Pd nanocrystals enclosed by high-index facets and thus enhanced catalytic activities (arising from high densities of atomic steps and kinks) have not succeeded until recently. To this end, Sun and co-workers demonstrated an electrochemical approach to the synthesis of Pd tetrahexahedra (greater than 60 nm in size) with high-index facets by applying a square-wave potential to a polycrystalline sample of Pd powders supported on an electrode.[3] Wang et al. reported the synthesis of gold–palladium core–shell nanocrystals with high-index facets by depositing Pd layers on Au tetrahexahedra or trisoctahedra by chemical reduction.[4]

Parallel to the aforementioned convex systems, nanocrystals with a concave structure on the surface have also received great attention for generating high-index facets.[5] To this end, we demonstrated the synthesis of Pd nanocubes with cavities on the surface through a wet etching process.[5a] Zheng and co-workers reported a solvothermal method for the synthesis of tetrahedral and trigonal bipyramidal Pd nanocrystals with cavities in the interiors by using formaldehyde as a reducing agent.[5b] Mirkin and co-workers demonstrated the synthesis of Au concave nanocubes enclosed by 24 high-index {730} facets by seeded growth with cetyltrimethylammonium chloride (CTAC) as a capping agent.[5c] Compared to the use of a special etching, reducing, or capping agent, kinetic control may represent a simpler and more powerful route to the facile synthesis of noble-metal nanocrystals with a concave structure on the surface. In general, a kinetically controlled synthesis can be achieved by controlling a set of reaction parameters, including reagent concentration, temperature, injection rate, addition of ionic species. For example, we have demonstrated the synthesis of Pt tetrahedra and octahedra with a concave surface using an overgrowth approach by varying the amount of a coordination ligand for the Pt ions.[6] Most recently, we reported a facile route to the synthesis of rhodium, platinum, or platinum–rhodium concave nanocubes by simply manipulating the reaction kinetics with a syringe pump to alter the injection rate of a salt precursor.[7] Skrabalak and co-workers demonstrated the synthesis of Au–Pd nanocubes with a concave structure by using a seed-mediated co-reduction method.[8] Despite these demonstrations, we still lack a simple and reliable method for the direct synthesis of Pd concave nanocubes with compact dimensions and in high purity, together with a potential for high-volume production.

Herein, we report a simple route based on seeded growth to the synthesis of Pd concave nanocubes bounded by high-index {730} facets, where Pd nanocubes were used as seeds for the reduction of a Pd precursor in an aqueous solution. The reduction kinetics were controlled by manipulating the concentrations of reagents, including Na_2PdCl_4, KBr, and ascorbic acid (AA). In general, reducing the concentrations of Na_2PdCl_4 and KBr or increasing the concentration of AA was found to be beneficial to the formation of Pd concave nanocubes. Owing to their high-index facets, the Pd concave nanocubes exhibited substantially enhanced catalytic activity relative to the conventional nanocubes enclosed by {100} facets towards electro-oxidation of formic acid and Suzuki coupling reaction.

In a typical synthesis, an aqueous solution of Na_2PdCl_4 was injected (with a pipette) into a mixture containing poly(vinyl pyrrolidone) (PVP), KBr, AA, and Pd seeds under magnetic stirring. The Pd seeds were nanocubes with an average side length of 18 nm (Figure S1, Supporting Information), which were prepared using a procedure reported by our group.[9] A closer examination indicates that a small portion of the cubes were somewhat elongated along one of the axes to form rectangular bars with aspect ratios (length to width) slightly larger than one. Since both the cubes and bars were enclosed by {100} facets, they are collectively called "nanocubes" for

[*] M. Jin, Dr. H. Zhang, Prof. Y. Xia
Department of Biomedical Engineering, Washington University
Saint Louis, MO 63130 (USA)
E-mail: xia@biomed.wustl.edu
M. Jin, Prof. Z. Xie
State Key Laboratory for Physical Chemistry of Solid Surfaces and Department of Chemistry, Xiamen University (People's Republic of China)
Dr. H. Zhang
State Key Laboratory of Silicon Materials and Department of Materials Science and Engineering, Zhejiang University (People's Republic of China)

[**] This work was supported in part by the NSF (DMR-0804088) and startup funds from Washington University in St. Louis. As a visiting student from Xiamen University, M.J. was also partially supported by the China Scholarship Council (CSC). Part of the work was performed at the Nano Research Facility (NRF), a member of the National Nanotechnology Infrastructure Network (NNIN), which is supported by the NSF under award no. ECS-0335765.

Supporting information for this article is available on the WWW under http://dx.doi.org/10.1002/anie.201103002.

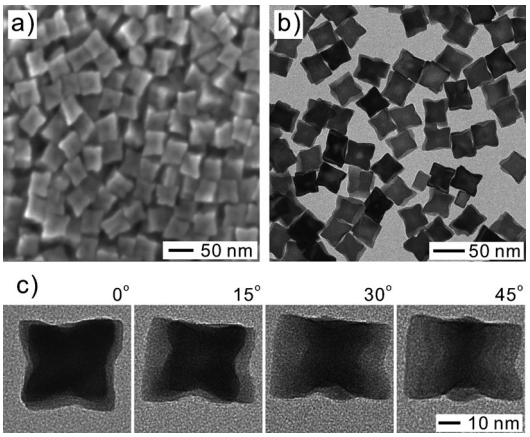

Figure 1. a) SEM and b) TEM images of Pd concave nanocubes that were prepared using the standard procedure. c) TEM images of a Pd concave nanocube recorded at different tilting angles.

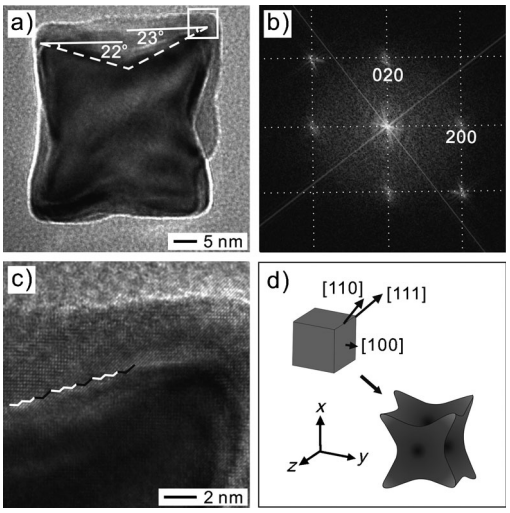

Figure 2. a) HRTEM image and b) the corresponding Fourier transform (FT) pattern of a Pd concave nanocube recorded along the [001] zone axis. c) HRTEM image of the corner region as marked by the white box in (a), where the white and black colors represented {420} and {310} facets, respectively. d) Schematic illustration of the formation of a Pd concave nanocube from a cubic seed by preferential overgrowth at the corners and edges.

simplicity. Figure 1 shows SEM and TEM images of Pd concave nanocubes prepared using the standard procedure. From the SEM image (Figure 1 a), it is clear that each face of the nanocube in the product was excavated by a square pyramid in the center. As shown by the TEM image in Figure 1 b, the cubic nanocrystal exhibited a darker contrast in the center than at the edges, thus confirming the formation of a concave structure on the surface. The TEM images obtained from a nanocube at different tilting angles (Figure 1 c) also support the formation of a concave rather than flat surface on each side face. Additional SEM images in Figure S2 in the Supporting Information demonstrate that the Pd concave nanocubes could be obtained in high purity (> 90 %) and relatively large quantity. In addition to the transition from a flat to a concave surface, the average edge length was found to increase from 18 to 37 nm during the overgrowth process.

For a concave nanocube enclosed by high-index facets, the Miller indices can be derived from the projection angles along a selected crystallographic axis.[10] Table S1 (Supporting Information) gives the angles for different types of high-index facets when they are projected along the [001] direction. Figure 2 a shows a high-resolution (HR) TEM image of an individual Pd concave nanocube viewed along the ⟨100⟩ zone axis, as confirmed by the corresponding Fourier transform (FT) pattern (Figure 2 b). Obviously, eight side faces of a concave cube can be projected edge-on from this orientation. By comparing the measured projection angles (Figure 2 a) with the calculated ones (Table S1 in the Supporting Information), these eight edge-on faces could be indexed as the {730} planes. The Miller indices of a high-index facet could also be determined from the arrangement of atoms on the edge-on projected face.[10] The edge-on projected face of a Pd concave nanocube in Figure 2 c shows a series of alternating {420} (white color) and {310} (black color) sub-facets, resulting in an overall profile indexed as the {730} planes. Figure S3 in the Supporting Information shows an atomic model of {730} planes with {100} terraces and {110} steps. On the basis of this structural analysis, the Pd concave nanocube was supposed to form by preferential overgrowth at corners and edges of a cubic seed along the ⟨111⟩ and ⟨110⟩ directions, respectively, as well as some slight growth on the {100} facets along the ⟨100⟩ directions (Figure 2 d).

To elucidate the mechanism involved in the formation of Pd concave nanocubes, we conducted a set of experiments using the standard procedure, except that different concentrations were used for the reagents, including Na_2PdCl_4, KBr, and AA. The results shown in Figure 3 indicate that the formation of Pd concave nanocubes was highly sensitive to the concentrations of these reagents. For Na_2PdCl_4 and KBr, lowering their concentrations (Figure 3 a, c) favored preferential overgrowth at corners and edges of the Pd cubic seeds and thus formation of concave nanocubes. In contrast, Pd nanocubes with flat faces were obtained when the concentrations of Na_2PdCl_4 (Figure 3 b) and KBr (Figure 3 d) were increased relative to those used in the standard procedure. When the concentration of Na_2PdCl_4 was increased (Figure 3 b) or the concentration of KBr was reduced (Figure 3 c), there was a tendency to form small Pd nanocubes through homogeneous nucleation. In contrast, the concentration of AA showed a different trend in influencing the formation of Pd concave nanocubes. In this case, increasing the concentration of AA (Figure 3 f) favored the formation of concave nanocubes as opposed to the case of lowering its concentration (Figure 3 e). Taken together, the growth habit of Pd cubic seeds could be readily controlled by varying the concentrations of Na_2PdCl_4, KBr, and AA to manipulate the reduction kinetics.

For a kinetically controlled synthesis, the diffusion rate (denoted by V_1) of precursor from solution to the surface and the growth rate (denoted by V_2) at which atoms are generated and added to the surface of a growing seed plays a critical role in determining the growth habit of a seed, as previously discussed by Chernov.[11] When V_1 is much larger than V_2, the concentration of precursor is identical in regions very close to

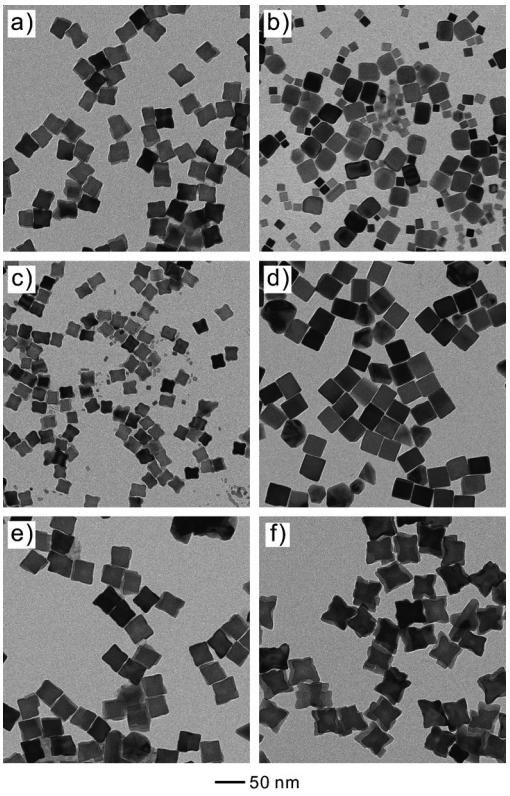

Figure 3. TEM images of Pd nanocrystals that were prepared using the standard procedure, except the variation in concentration for the reagent listed below: a) 7.2 and b) 59.0 mg Na_2PdCl_4; c) 30 and d) 1200 mg KBr; and e) 30 and f) 120 mg ascorbic acid.

the surface of a seed and far away from the seed owing to fast diffusion. An atom derived from a precursor molecule can be added to different sites on a seed with equal probability, and hence preferential overgrowth is not supported under this condition. When V_1 is much smaller than V_2, however, there will be a gradient for the precursor concentration by which the concentration decreases when moving from the bulk solution towards the surface of a seed. As such, the atom generated on the surface of a seed will be preferentially added to the site with the highest reactivity owing to an insufficient supply of atoms. Herein, the concentrations of Na_2PdCl_4, KBr, and AA were adjusted to manipulate V_1 and V_2 and thus the growth habit of Pd cubic seeds. Specifically, reducing the concentration of Na_2PdCl_4 will slow down V_1, and reducing the concentration of KBr will speed up V_2 owing to a fast reduction rate for $[PdCl_4]^{2-}$ relative to $[PdBr_4]^{2-}$.[12] On the other hand, increasing the concentration of AA (the reducing agent) will always increase V_2. Taken together, preferential overgrowth on the seeds is expected when the concentrations of Na_2PdCl_4 and KBr are reduced or the concentration of AA is increased.

For a cubic seed, the reactivity of different sites is supposed to decrease in the order of corner, edge, and side face. This difference in reactivity can be further amplified by the presence of Br^- ions that can selectively adsorb onto the {100} facets and thus slow down the growth rate of a side face. As a result, at low concentrations of Na_2PdCl_4 and KBr or high concentrations of AA, V_1 will be much smaller than V_2, and the new Pd atoms will be preferentially added to the corners and edges of a Pd cubic seed, thus resulting in the formation of a concave nanocube. This observation is different from the result recently reported for the synthesis of Pt concave nanocubes in the presence of KBr.[7b] The difference can be attributed to the use of different reducing agents. For the Pt system, Pt atoms were immediately formed in the solution phase by reduction of the Pt precursor with a strong reducing agent such as $NaBH_4$, and then added to the surface of a growing Pt seed. In the case of Pd, the Na_2PdCl_4 precursor had to diffuse to the surface (or at least to the vicinity of the surface) of a growing Pd seed and then be reduced into Pd atoms owing to the use of a relatively weak reducing agent AA. As a result, the dependency of growth behavior on the concentration of reducing agent showed opposite trends in these two systems.

Palladium nanocubes of other different sizes were also employed as the seeds to grow Pd concave nanocubes. Figure S4 (Supporting Information) shows TEM images of Pd nanocubes of 10 and 6 nm in edge length that were used as seeds, and their corresponding Pd concave nanocubes. The results indicate that Pd concave nanocubes with sizes of 27 and 15 nm could still be obtained by preferential overgrowth at corners and edges of the seeds. The results also suggest that the size of the Pd concave nanocubes could be controlled over a broad range by simply using Pd nanocubes with different sizes as the seeds. For the 15 nm Pd concave nanocubes obtained from the 6 nm seeds, the purity and uniformity still need to be improved by optimizing the concentrations for the reagents. In general, cubic seeds of large sizes will be beneficial to the formation of high-quality concave nanocubes, as the concentration gradient on a large cube will be greater than that on a small one.

The Pd concave nanocubes 37 nm in size with {730} facets exposed on the surface were then evaluated as catalysts for electro-oxidation of formic acid. We benchmarked the electrocatalytic activity of these concave nanocubes against the conventional Pd nanocubes enclosed by {100} facets and with an average size of 37 nm. According to previous work, the catalytic activity of metal catalysts could be affected by different capping agents.[13] However, since both the conventional and concave nanocubes were synthesized using similar methods (except the use of reagents at different concentrations), their surfaces should be capped by similar chemical groups, PVP and Br^- ions. As such, we could directly compare their activities to single out the influence of atomic structure on the surface. In the first step, the electrochemically active surface area (ECSA) of the Pd nanocrystals was determined from the charges associated with the stripping of a Cu monolayer underpotentially deposited (UPD) on their surface,[14] as shown in Figure S5 in the Supporting Information. Figure 4 shows cyclic voltammograms normalized against the ECSAs of these two catalysts for electro-oxidation of formic acid at room temperature in a 150 mL solution containing 0.1 M $HClO_4$ and 2 M HCOOH. It is clear that the Pd concave nanocubes exhibited higher electro-catalytic activity than the conventional nanocubes, with a 1.9 times increase for the peak current. We believe that the high-index {730} facets with a

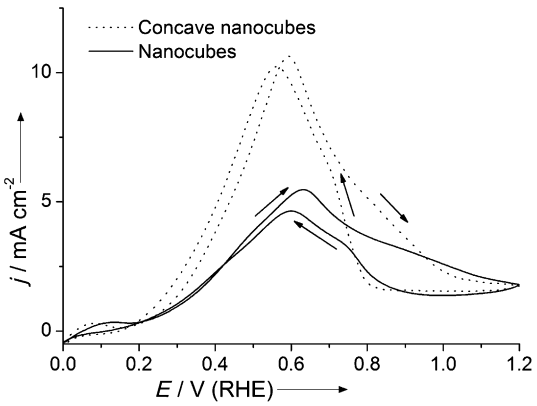

Figure 4. Cyclic voltammograms of the Pd nanocubes enclosed by concave or flat faces, which were recorded at room temperature in a solution containing 2 M HCOOH and 0.1 M $HClO_4$ at a sweep rate of 50 $mV s^{-1}$. The current density was normalized against the corresponding ECSA. RHE = reversible hydrogen electrode.

higher density of low-coordinate atomic steps and kinks were responsible for the enhanced activity for formic acid oxidation. Besides this high surface activity generated from high-index facets, the mass activity of Pd concave nanocubes can be further enhanced by reducing the size of the nanocrystals (see Figure S6 in the Supporting Information).

The Pd concave nanocubes 37 nm in size were also tested as catalysts for the Suzuki coupling reaction, which was performed using a procedure similar to what was described in literature.[4] In the reaction (Figure S7 in the Supporting Information), phenylboronic acid is coupled with iodobenzene to form biphenyl over the Pd catalyst. In the absence of a Pd catalyst, no biphenyl was detected in the reaction, indicating that the Pd-containing nanocrystals were indispensable for the coupling reaction. For each catalyst, the coupling reaction was carried out three times under the same conditions. Table 1 compares the catalytic properties of the Pd nanocubes with a concave or flat surface for Suzuki coupling reaction. For the Pd concave nanocubes, 99% iodobenzene was converted into biphenyl after 20 min. In comparison, a conversion yield of 38% was obtained for the conventional nanocubes. When recycled one time, the conversion yield for the Pd concave nanocubes was still as high as 96%. The intrinsic turnover frequency (TOF, defined here as the iodobenzene conversion per surface Pd atom per second) of the catalyst was obtained from the total number of surface Pd atoms (see the Supporting Information for details). As shown in Table 1, the TOF of the Pd concave nanocubes was $11.3\ s^{-1}$, which was 3.5 times higher than that of the conventional Pd nanocubes ($3.2\ s^{-1}$). Significantly, the Pd nanocrystals in both catalysts maintained their morphologies during the catalytic reaction, as revealed by TEM imaging (Figure S8 in the Supporting Information).

Table 1: Conversion yields and TOFs per surface Pd atom for Suzuki coupling reaction with the use of Pd nanocubes enclosed by a concave or flat surface as the catalyst.

Palladium catalyst	Yield [%]	Number of surface atoms	TOF [s^{-1}]
concave cubes	99 ± 1	1.35×10^{16}	11.3 ± 0.1
recycled concave cubes	96	1.35×10^{16}	10.8
conventional cubes	38 ± 2	1.79×10^{16}	3.2 ± 0.1
recycled cubes	33	1.79×10^{16}	2.8

In summary, we have demonstrated a facile synthesis of Pd concave nanocubes enclosed by high-index {730} facets through preferential overgrowth on Pd cubic seeds. The key was to induce preferential overgrowth at corners and edges of a cubic seed by lowering the concentrations of Na_2PdCl_4 and KBr or increasing the concentration of AA. Otherwise, the Pd cubic seeds would grow into larger cubes enclosed by {100} facets when the overgrowth took no preference along different crystallographic directions. When compared with the conventional Pd nanocubes enclosed by low-index {100} facets, the Pd concave nanocubes exhibited substantially enhanced catalytic activities towards electro-oxidation of formic acid and in the Suzuki coupling reaction. This approach based on kinetically controlled overgrowth can potentially be extended to other noble metals to generate nanocrystals with high-index facets and thus high activities towards various types of reactions.

Received: May 1, 2011
Published online: July 5, 2011

Keywords: crystal growth · high-index facets · kinetic control · nanoparticles · palladium

[1] a) H. Meng, S. Sun, J. Masse, J. Dodelet, *Chem. Mater.* **2008**, *20*, 6998–7002; b) Z. Bai, L. Yang, L. Li, J. Lv, K. Wang, J. Zhang, *J. Phys. Chem. C* **2009**, *113*, 10568–10573; c) X. Huang, S. Tang, X. Mu, Y. Dai, G. Chen, Z. Zhou, F. Ruan, Z. Yang, N. Zheng, *Nat. Nanotechnol.* **2011**, *6*, 28–32.

[2] a) Y. Xiong, J. McLellan, J. Chen, Y. Yin, Z. Li, Y. Xia, *J. Am. Chem. Soc.* **2005**, *127*, 17118–17127; b) B. Lim, Y. Xiong, Y. Xia, *Angew. Chem.* **2007**, *119*, 9439–9442; *Angew. Chem. Int. Ed.* **2007**, *46*, 9279–9282; c) Y. Xiong, H. Cai, B. Wiley, J. Wang, M. Kim, Y. Xia, *J. Am. Chem. Soc.* **2007**, *129*, 3665–3675; d) Y. Xiong, H. Cai, Y. Yin, Y. Xia, *Chem. Phys. Lett.* **2007**, *440*, 273–278.

[3] a) N. Tian, Z. Zhou, S. Sun, *Chem. Commun.* **2009**, 1502–1504; b) N. Tian, Z. Zhou, N. Yu, L. Wang, S. Sun, *J. Am. Chem. Soc.* **2010**, *132*, 7580–7581.

[4] F. Wang, C. Li, L. Sun, H. Wu, T. Ming, J. Wang, J. Yu, C. Yan, *J. Am. Chem. Soc.* **2011**, *133*, 1106–1111.

[5] a) H. Zhang, M. Jin, J. Wang, W. Li, P. H. C. Camargo, M. J. Kim, D. Yang, Z. Xie, Y. Xia, *J. Am. Chem. Soc.* **2011**, *133*, 6078–6089; b) X. Huang, S. Tang, H. Zhang, Z. Zhou, N. Zheng, *J. Am. Chem. Soc.* **2009**, *131*, 13916–13917; c) J. A. Zhang, M. R. Langille, M. L. Personick, K. Zhang, S. Li, C. A. Mirkin, *J. Am. Chem. Soc.* **2010**, *132*, 14012–14014; d) J. Zhang, L. Zhang, S. Xie, Q. Kuang, X. Han, Z. Xie, L. Zheng, *Chem. Eur. J.* **2011**, DOI: 10.1002/chem.201103002.

[6] T. Herricks, J. Chen, Y. Xia, *Nano Lett.* **2004**, *4*, 2367–2371.

[7] a) H. Zhang, W. Li, M. Jin, J. Zeng, T. Yu, D. Yang, Y. Xia, *Nano Lett.* **2011**, *11*, 898–903; b) T. Yu, D. Kim, H. Zhang, Y. Xia, *Angew. Chem.* **2011**, *123*, 2825–2829; *Angew. Chem. Int. Ed.* **2011**, *50*, 2773–2777.

[8] C. DeSantis, A. Peverly, D. Peters, S. Skrabalak, *Nano Lett.* **2011**, *11*, 2164–2168.

[9] M. Jin, H. Liu, H. Zhang, Z. Xie, J. Liu, Y. Xia, *Nano Res.* **2011**, *4*, 83 – 91.
[10] a) N. Tian, Z. Zhou, S. Sun, Y. Ding, Z. Wang, *Science* **2007**, *316*, 732 – 735; b) N. Tian, Z. Zhou, S. Sun, *J. Phys. Chem. C* **2008**, *112*, 19801 – 19817.
[11] A. Chernov, *Sov. Phys. Cryst.* **1972**, *16*, 734 – 753.
[12] a) S. Srivastava, L. Newman, *Inorg. Chem.* **1966**, *5*, 1506 – 1510; b) S. Feldberg, P. Klotz, L. Newman, *Inorg. Chem.* **1972**, *11*, 2860 – 2865.
[13] J. Kuhn, C. Tsung, W. Huang, G. Somorjai, *J. Catal.* **2009**, *265*, 209 – 215.
[14] a) T. Chierchie, C. Mayer, *Electrochim. Acta* **1988**, *33*, 341 – 345; b) J. Okada, J. Inukai, K. Itaya, *Phys. Chem. Chem. Phys.* **2001**, *3*, 3297 – 3302.